Inorg. Chem. **2006**, *45*, 9798–9811

Metal Binding to Bipyridine-Modified PNA

Raphael M. Franzini,[†] Richard M. Watson,[†] Goutam K. Patra,[†] Robert M. Breece,[‡] David L. Tierney,[‡] Michael P. Hendrich,[†] and Catalina Achim*[,†]

Department of Chemistry, Carnegie Mellon University, 4400 5th Avenue, Pittsburgh, Pennsylvania 15213, and Department of Chemistry, University of New Mexico, Albuquerque, New Mexico 87131

Received May 31, 2006

Substitution of natural nucleobases in PNA oligomers with ligands is a strategy for directing metal ion incorporation to specific locations within a PNA duplex. In this study, we have synthesized PNA oligomers that contain up to three adjacent bipyridine ligands and examined the interaction with Ni^{2+} and Cu^{2+} of these oligomers and of duplexes formed from them. Variable-temperature UV spectroscopy showed that duplexes containing one terminal pair of bipyridine ligands are more stable upon metal binding than their nonmodified counterparts. While binding of one metal ion to duplexes that contain two adjacent bipyridine pairs makes the duplexes more stable, additional metal ions lower the duplex stability, with electrostatic repulsions being, most likely, an important contributor to the destabilization. UV titrations showed that the presence of several bipyridine ligands in close proximity of each other in PNA oligomers exerts a chelate effect. A supramolecular chelate effect occurs when several bipyridines are brought next to each other by hybridization of PNA duplexes. EPR spectroscopy studies indicate that even when two Cu^{2+} ions coordinate to a PNA duplex in which two bipyridine pairs are next to each other, the two metal–ligand complexes that form in the duplex are far enough from each other that the dipolar coupling is very weak. EXAFS and XANES show that the Ni^{2+}-bipyridine bond lengths are typical for $[Ni(bipy)_2]^{2+}$ and $[Ni(bipy)_3]^{2+}$ complexes.

Introduction

The combined use of the hybridization properties of nucleic acids with the coordinative properties of the transition metal ions is a promising route to metal-containing nanostructures. The potential applications of these structures are either to expand the genetic code by storing and reading information into a sequence of metal complexes or to create supermolecules with specific magnetic or electronic properties. The rational incorporation of transition metal ions at predefined positions within nucleic acid duplexes can be achieved by substitution of pairs of complementary nucleobases with ligands. Generally, the metal ions coordinate to four-dentate binding sites of the type [2 + 2] or [3 + 1] to create square planar complexes, whose aromatic ligands are involved in π-stacking interactions with the adjacent nucleobases. Since 1999 when this strategy was first proposed,[1] several groups have applied it to create DNA,[2−8] peptide nucleic acid (PNA),[9−12] locked nucleic acid (LNA),[13] or glycol nucleic acid (GNA) duplexes[14] that contain various transition metal ions.

* To whom correspondence should be addressed. E-mail: achim@cmu.edu.
[†] Carnegie Mellon University.
[‡] University of New Mexico.

(1) Tanaka, K.; Shionoya, M. *J. Org. Chem.* **1999**, *64*, 5002−5003.
(2) Zimmermann, N.; Meggers, E.; Schultz, P. G. *Bioorg. Chem.* **2004**, *32*, 13−25.
(3) Zimmermann, N.; Meggers, E.; Schultz, P. G. *J. Am. Chem. Soc.* **2002**, *124*, 13684−13685.
(4) Atwell, S.; Meggers, E.; Spraggon, G.; Schultz, P. G. *J. Am. Chem. Soc.* **2001**, *123*, 12364−12367.
(5) Meggers, E.; Holland, P. L.; Tolman, W. B.; Romesberg, F. E.; Schultz, P. G. *J. Am. Chem. Soc.* **2000**, *122*, 10714−10715.
(6) Tanaka, K.; Tengeiji, A.; Kato, T.; Toyama, N.; Shiro, M.; Shionoya, M. *J. Am. Chem. Soc.* **2002**, *124*, 12494−12498.
(7) Tanaka, K.; Yamada, Y.; Shionoya, M. *J. Am. Chem. Soc.* **2002**, *124*, 8802−8803.
(8) Weizman, H.; Tor, Y. *Chem. Commun.* **2001**, 453−454.
(9) Watson, R. M.; Skorik, Y. A.; Patra, G. K.; Achim, C. *J. Am. Chem. Soc.* **2005**, *127*, 14628−14639.
(10) Popescu, D.-L.; Parolin, T. J.; Achim, C. *J. Am. Chem. Soc.* **2003**, *125*, 6354−6355.
(11) Küsel, A.; Zhang, J.; Gil, M. A.; Stueckl, A. C.; Meyer-Klaucke, W.; Meyer, F.; Diederichsen, U. *Eur. J. Inorg. Chem.* **2005**, 4317−4324.
(12) Franzini, R.; Watson, R. M.; Popescu, D.-L.; Patra, G. K.; Achim, C. *Polym. Prepr.* **2004**, *45*, 337−338.
(13) Babu, B. R.; Hrdlicka, P. J.; McKenzie, C. J.; Wengel, J. *Chem. Commun.* **2005**, 1705−1707.
(14) Zhang, L.; Meggers, E. *J. Am. Chem. Soc.* **2005**, *127*, 74−75.

10.1021/ic0609610 CCC: $33.50
Published on Web 11/04/2006

Scheme 1. Cartoon Representations of Possible Structures of Metal-Containing **Bpy**−PNA Duplexes[a]

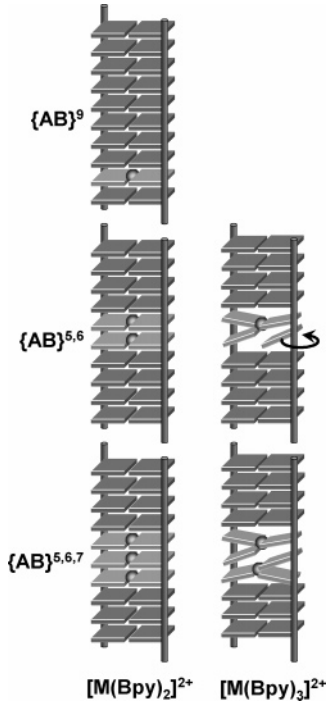

[a] These cartoons are not meant to indicate the actual geometry of the metal center or distortions of nearby nucleobases. Structures are composed of the PNA backbone (dark rods), natural nucleobases (dark plates), **Bpy** (light plates), and M^{2+} ions (silver spheres). For specific PNA sequences, see Chart 1.

A significantly smaller number of duplexes that contain multiple metal-binding sites have been reported. To date, Schultz et al. have incorporated two isolated neutral copper complexes with mixed pyridine:pyridine-2,6-dicarboxylate coordination into a 12-bp DNA duplex and obtained a crystal structure of the metal-containing duplex.[4] Shionoya has demonstrated the incorporation of five neutral copper−hydroxypyridone moieties between two end-of-duplex natural DNA basepairs by UV titrations and EPR spectroscopy.[15] Zimmerman et al. have reported a stabilization effect of a stoichiometric amount of metal ions when two or four adjacent ligand pairs of [3 + 1] type have been incorporated in adjacent positions in 15-bp DNA duplexes.[2] The thermal stability of DNA duplexes that contain three pairs of neutral, bidentate ligands has been reported to be maximum in the presence of 3 equiv of Ni^{2+}, suggesting that up to three positively charged metal−ligand complexes can form in DNA duplexes.[16] Given the presence of several high-affinity metal-binding sites within a duplex, the formation of multiple, stacked metal base pairs is only one of several modes of coordination (Scheme 1). Therefore, we decided to systematically investigate the metal binding to peptide nucleic acid duplexes that contain several ligands and can act as scaffolds for multiple metal ions.

In a previous study, we replaced an A:T base pair in the middle of a PNA duplex {**AB**} with two bipyridine ligands

Chart 1. Sequences and Numbering Scheme for PNA Oligomers and Duplexes.

{AB}

1 2 3 4 **5** 6 7 8 **9** 10

H-GTAG**A**TCA**C**T-Lys-NH_2 **A**

H_2N-Lys-CATC**T**AGT**G**A-H **B**

10 9 8 7 **6** 5 4 3 **2** 1

{AB}^{5}

H-GTAG**Bpy**TCACT-Lys-NH_2 **A^5**

H_2N-Lys-CATC**Bpy**AGTGA-H **B^6**

{AB}^{9}

H-GTAGATCA**Bpy**T-Lys-NH_2 **A^9**

H_2N-Lys-CATCTAGT**Bpy**A-H **B^2**

{A^5:B^{5,6}}

H-GTAG**Bpy**TCACT-Lys-NH_2 **A^5**

H_2N-Lys-CATC**Bpy****Bpy**GTGA-H **B^{5,6}**

{AB}^{5,6}

H-GTAG**Bpy****Bpy**CACT-Lys-NH_2 **A^{5,6}**

H_2N-Lys-CATC**Bpy****Bpy**GTGA-H **B^{5,6}**

{AB}^{5,6,7}

H-GTAG**Bpy****Bpy****Bpy**ACT-Lys-NH_2 **A^{5,6,7}**

H_2N-Lys-CATC**Bpy****Bpy****Bpy**TGA-H **B^{4,5,6}**

Partial Self-Complementarity of A^{5,6}:

A

H-GT|G**Bpy****Bpy**CACT-Lys-NH_2 **A^{5,6}**

H_2N-Lys-TCAC**Bpy****Bpy**G|TG-H **A^{5,6}**

A

situated in complementary positions[10,12] {**AB**}^{5} (Chart 1) and showed that Ni^{2+} binds to the ligands and increases the stability of the bipyridine-modified duplex, compared to that of the metal-free duplex. Here, we report how the effect of metal ions on the duplex stability depends on where in the duplex the metal is situated. We also show that Cu^{2+} and Co^{2+} coordinate to bipyridine-substituted PNA duplexes. Finally, incorporation of more than two bipyridine ligands in adjacent positions within the PNA duplex allowed us to bind multiple metal ions to the same duplex. The properties of these duplexes before and after metal incorporation have been studied using optical and EPR spectroscopy, EXAFS and XANES.

Results and Discussion

PNA Monomer and Oligomer Synthesis. The carboxymethylated bipyridine nucleobase **1** was coupled to the protected aminoethyl-glycine **2** to obtain the PNA monomer ester **3**, which was subsequently hydrolyzed to obtain the PNA monomer acid **4** (Scheme 2). This monomer was used in the solid-phase synthesis of the PNA oligomers using standard Boc protection.[17] The oligomers were purified by reverse-phase HPLC and analyzed by MALDI-TOF mass spectrometry. The sequences of oligomers used in this study are summarized in Chart 1. In these sequences and elsewhere, **Bpy** denotes the bipyridine PNA monomer contained in PNA oligomers and bipy denotes the unattached 2,2′-bipyridine ligand.

(15) Tanaka, K.; Tengeiji, A.; Kato, T.; Toyama, N.; Shionoya, M. *Science* **2003**, *299*, 1212−1213.
(16) Switzer, C.; Sinha, S.; Kim, P. H.; Heuberger, B. D. *Angew. Chem., Int. Ed.* **2005**, *44*, 1529−1532.
(17) Nielsen, P. E., Ed. *Peptide Nucleic Acids: Protocols and Applications*, 2nd ed.; Horizon Bioscience: Hethersett, Norwich, U.K., 2004.

Scheme 2. Synthesis of the Bipyridine−PNA Monomer **Bpy**[a]

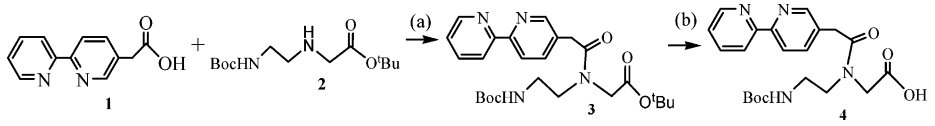

[a] (a) DCC, DhbtOH, DCM, DMF; (b) NaOH, CH_2H_5OH, H_2O.

Table 1. Melting Temperatures for Bipyridine-Containing PNA Duplexes (°C)[a]

		Ni^{2+}		Co^{2+}		Cu^{2+}	
	none	1 equiv	2 equiv	1 equiv	2 equiv	1 equiv	2 equiv
{**AB**}	66	66	−	66	−	67	−
{**AB**}^{5}	44	58	−	50	−	48	−
{**AB**}^{9}	65	>85	−	78	−	75	−
{**AB**}^{5,6}	37	57	45	50	45	42	37

[a] − indicates not measured. Precision is ±1 °C for all values except those measured for {**AB**}^{5,6}-based duplexes for which it is ±3 °C because of broad transitions.

Thermal Stability of PNA Duplexes Containing Bpy Pairs. Thermal denaturation experiments were performed for the duplexes listed in Chart 1 in the absence and presence of transition metal ions. The bipyridine PNA monomer used in our previous studies contained a 5-methyl-substituent (**Me-Bpy**).[10] In the experiments reported in the present paper, we have used the unsubstituted bipyridine monomer **Bpy**. Importantly, the melting behavior of the {**AB**}^{5} duplex in the presence of Ni^{2+} was the same as that for the analogous PNA duplex that contained **Me-Bpy** monomers in place of **Bpy**. This indicates that the methyl group does not exert a measurable steric or electronic effect on the metal binding to the duplex.

The duplex {**AB**}^{9} contains two bipyridine ligands in place of an A:T base pair near the end of the duplex. The melting temperature (T_M) of this duplex in the absence of metal ions is nearly identical to that of the nonmodified duplex {**AB**} (Table 1). In contrast, replacement of a central A:T base pair with a pair of **Bpy** (as in {**AB**}^{5}) or **Me-Bpy** ligands[10] reduced the duplex stability drastically. The influence of the position of ligand substitution on the duplex stability can be explained by the fact that terminal base pairs have a higher tendency for fraying than the central ones. Thus, mismatches or substitution of base pairs with ligand pairs that cannot form hydrogen bonds have a smaller influence on the duplex stability when situated near the duplex terminus than when placed in the middle of the duplex.

The melting temperature of {**AB**}^{5,6}, which contains two adjacent **Bpy** pairs, is lower than that of the duplexes that contain a single pair of bipyridines (Figure 1a and Table 1). Furthermore, a decrease in the absorbance at 260 nm occurs upon slow cooling of a 1:1 mixture of **A**^{5,6,7} and **B**^{4,5,6} from 95 to 15 °C, but the absorption does not reach a plateau (Figure 1a), which suggests that the duplex {**AB**}^{5,6,7} is not completely formed at 15 °C. Therefore, the duplex melting temperature must be lower than 30 °C. The loss of thermal stability of duplexes with an increasing number of bipyridine pairs can be rationalized by the fact that two bipyridines situated across from each other in the duplex cannot form hydrogen bonds and are not size complementary. This result is in agreement with that of Brotschi et al., who have incorporated up to seven bipyridine pairs in the middle of DNA duplexes and have observed that the stability of the duplexes decreased with an increasing number of bipyridine pairs.[18] The decrease observed upon incorporation of a bipyridine pair into a DNA duplex is smaller than that observed by us for a PNA duplex, which correlates with the superior mismatch discrimination of PNA over DNA.

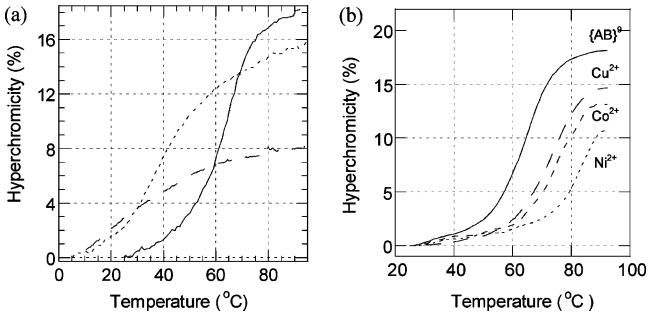

Figure 1. Melting curves measured for (a) 5 μM {**AB**}^{9} (solid line), {**AB**}^{5,6} (dotted line), and {**AB**}^{5,6,7} (dashed line) in the absence of transition metal ions and (b) 5 μM {**AB**}^{9} duplexes in the absence and presence of 1 equiv of Ni^{2+}, Cu^{2+}, or Co^{2+}. Solutions were prepared in pH 7, 10 mM sodium phosphate buffer.

The addition of metal ions increases the melting temperature of {**AB**}^{9} (Figure 1b and Table 1); the stabilization decreases from Ni^{2+} (ΔT_M > 20 °C) to Co^{2+} (ΔT_M = 13 °C) and Cu^{2+} (ΔT_M = 10 °C). This trend correlates with the binding constant to bipy being largest for Ni^{2+} and the ionic radius being smallest for Ni^{2+} (Table S1). The effect of metal binding on T_M is larger for {**AB**}^{9} than for {**AB**}^{5}.[10] The larger ΔT_M is likely a consequence of the fact that the metal complex situated close to the end of {**AB**}^{9} replaces an A:T nucleobase pair that is subject to fraying. Also, in the [M(**Bpy**)$_2$] complexes formed within the duplex, the two bipyridine ligands cannot be strictly coplanar because of steric interactions between the 6 and 6′ protons of the two ligands (Scheme 3), and this deviation from planarity for the metal−ligand complex is likely to have a lower destabilization effect when the complex is situated at the end of the PNA duplex. The UV spectra for {**AB**}^{9} duplexes (Figure S1) in the presence of Co^{2+}, Ni^{2+}, or Cu^{2+} reveal that the metal ions coordinate to bipyridine at low temperature. At high temperature, the latter two metal ions remain at least partially bound to bipyridine-modified PNA oligomers, while Co^{2+} is not bound (Figure S1). The difference between the behaviors of these metal ions is in agreement with the relative order of their binding constants for bipyridine (Table S1).

The addition of 1 equiv of metal ions increases the thermal stability of the {**AB**}^{5,6} duplex (Figure S2 and Table 1); the

(18) Brotschi, C.; Mathis, G.; Leumann, C. J. *Chem.−Eur. J.* **2005**, *11*, 1911−1923.

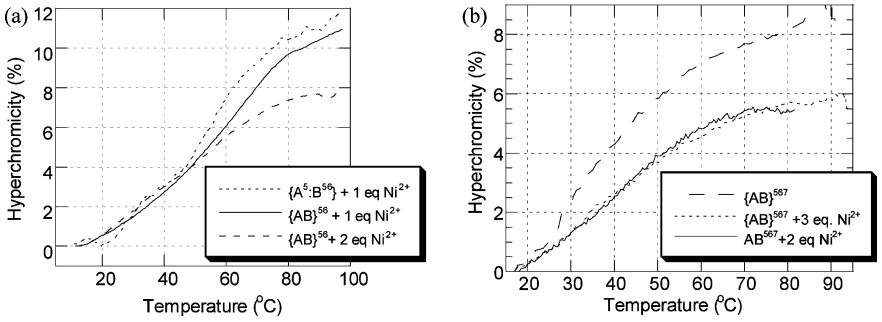

Figure 2. Melting curves measured for (a) 5 μM {**AB**}^{5,6} in the presence of 1 or 2 equiv of Ni^{2+} and (b) 5 μM {**AB**}^{5,6,7} in the absence of transition metal ions and in the presence of 2 or 3 equiv of Ni^{2+}. Solutions were prepared in pH 7, 10 mM sodium phosphate buffer and transitions were monitored at 260 nm.

Scheme 3. Typical Distortions in $[M(bipy)_2]^{2+}$ Complexes

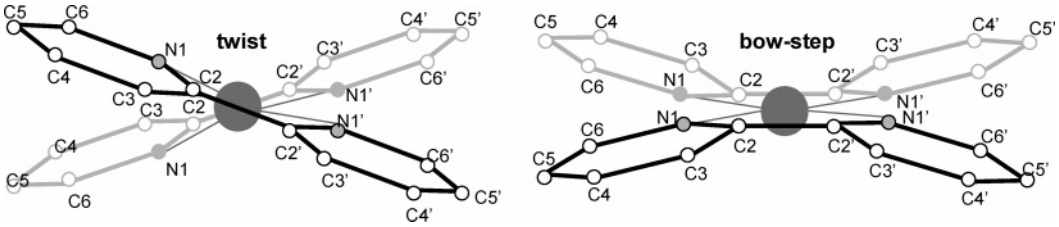

effect is again strongest for Ni^{2+} (ΔT_M = 20 °C). In the presence of 2 equiv of Ni^{2+}, the melting temperature of {**AB**}^{5,6} is 45 °C, which is between those measured for {**AB**}^{5,6} in absence of metal ions (T_M = 37 °C) and in the presence of 1 equiv of Ni^{2+} (T_M = 57 °C) (Table 1). The melting transitions in the presence of 1 equiv of metal ion are also steeper than in the presence of 2 equiv, indicating a more cooperative transition (Figure S2). The decrease in thermal stability of {**AB**}^{5,6} upon addition of a second equivalent of metal may be caused in part by electrostatic repulsion between the two metal ions situated in close proximity to each other. Second, the two bipyridines situated next to each other within the single stranded **A**^{5,6} or **B**^{5,6} create a four-dentate, high-affinity metal binding site, which can coordinate a metal ion even if no duplex is formed (see next section). If both bipyridine ligands present within each oligomer coordinated to a metal ion before strand association into a PNA duplex, coordination of two metal ions would not contribute to the enthalpy of duplex formation. This hypothesis is supported by the fact that no change in absorbance is observed at 315 nm, which is the $\pi-\pi^*$ band of the coordinated bipyridine, when {**AB**}^{5,6} duplexes are annealed from 95 to 20 °C in the presence of 2 equiv of metal ions (data not shown). Furthermore, the melting curve for the {**A**^{5}:**B**^{5,6}} duplex (Chart 1) in the presence of one equivalent of Ni^{2+}, which contains three bipyridines and a thymine instead of four bipyridines, is similar to that measured for the {**AB**}^{5,6} duplex under similar conditions (Figure 2a).

A hyperchromic change is observed at 260 nm for {**AB**}^{5,6,7} in the presence of 3 equiv of Ni^{2+}, Co^{2+}, or Cu^{2+}, but only an upper limit can be determined for the melting temperature, namely, T_M < 40 °C, because the duplex formation is not complete at 15 °C (Figure 2b). Interestingly, the melting curves measured for {**AB**}^{5,6,7} in the presence of 2 or 3 equiv of Ni^{2+} are identical (Figure 2b), suggesting that the third equivalent of metal ion does not interact with the PNA duplex.

Stoichiometry of Metal Binding to PNA Duplexes that Contain a Pair of Bpy Ligands. The dominant feature of the UV spectra of the nonmodified and bipyridine-modified PNA duplexes at both low and high temperature is the broad, intense, 260 nm absorption band attributed to the nucleobases (Figure S1a). Metal coordination to bipyridine shifts the $\pi-\pi^*$ bands of the ligand from 235 and 280 nm to 245 and 295−320 nm (Figure S1b and c and Table S2).[19,20] The absorption band at 295−320 nm is the only one not obscured by the nucleobase absorption.

Titrations with Ni^{2+} or Cu^{2+} of {**AB**}^{9} duplexes, which contain a pair of bipyridine ligands in complementary positions at the end of the duplex, show isosbestic points at 265 and 295 nm (Figure 3a and c). An inflection point is observed in the plots of absorption versus metal concentration for M^{2+}:{**AB**}^{9} = 1:1 (Figures 3b,d). The absorption coefficient at 310 nm for the complexes formed after the addition of 1 equiv of Ni^{2+} or Cu^{2+} is 27 000 or 26 700 M^{-1} cm^{-1}, respectively, which is close to the average of coefficients for $[Ni(bipy)]^{2+}$ and $[Ni(bipy)_3]^{2+}$ (i.e., 28 000 M^{-1} cm^{-1}, Table S2). These results indicate that both metal ions coordinate to the pair of **Bpy** ligands, which is in agreement with our previous finding that a $[Ni(\mathbf{Bpy})_2]^{2+}$ complex forms in the middle of {**AB**}^{5} duplexes.[10] Absorption changes observed at Cu^{2+}:{**AB**}^{9} ratios larger than 1:1 (Figures 3d and S3) suggest that the $[Cu(\mathbf{Bpy})_2]^{2+}$ complex originally formed in the duplex is transformed into $[Cu(\mathbf{Bpy})]^{2+}$ complexes in the presence of excess Cu^{2+}.

(19) Jorgensen, C. K. *Adv. Chem. Phys.* **1963**, *5*, 33−146.
(20) Sone, K.; Krumholz, P.; Stammreich, H. *J. Am. Chem. Soc.* **1955**, *77*, 777−780.

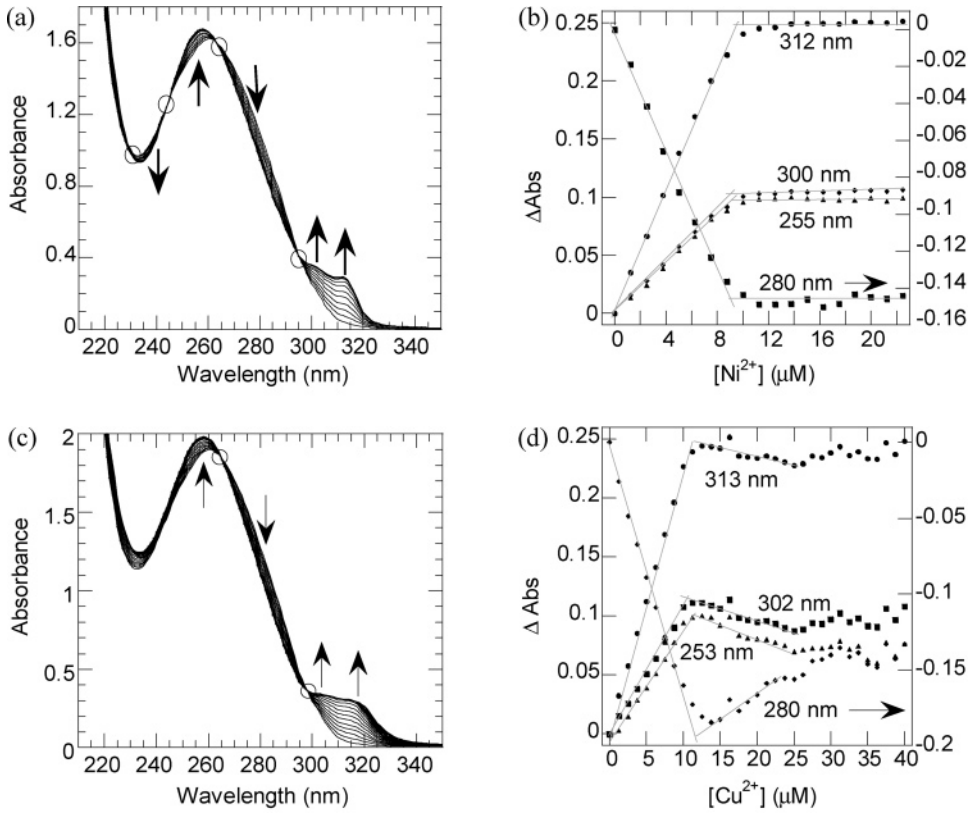

Figure 3. Spectrophotometric titration of 10 μM {**AB**}^{9} solutions in pH 7, 10 mM sodium phosphate buffer with Ni^{2+} (a and b) or Cu^{2+} (c and d).

Stoichiometry of Metal Binding to Bpy−PNA Strands Containing Two Pairs of Bpy Ligands. The presence of several ligands in close proximity to each other within the bipyridine-modified PNA oligomers and duplexes and the ability of the metal ions to coordinate one, two, or three bidentate ligands make possible the binding to these oligomers of multiple metal ions with different coordination modes, such as four-coordinate square planar or six-coordinate octahedral (Scheme 1). To distinguish between the potential complexes that may form in PNA duplexes that contain more than one pair of bipyridine ligands, we have titrated {**AB**}^{5,6} and {**AB**}^{5,6,7} with Cu^{2+} or Ni^{2+}.

Titration curves for the {**AB**}^{5,6} duplex with Ni^{2+} show an inflection point at a 1:1 Ni^{2+}:{**AB**}^{5,6} ratio (Figure 4a and b). The absorption coefficient at 310 nm of the species formed at the 1:1 inflection point calculated based on the Ni^{2+} concentration is 40 800 M^{-1} cm^{-1} (Table 2), which is similar to that reported for the synthetic complex $[Ni(bipy)_3]^{2+}$ (Table S2).[19] An inflection point for the change in absorption at 280 nm is also observed at one equivalent of Cu^{2+} per {**AB**}^{5,6} duplex (Figure 4d). This indicates that for both Ni^{2+} and Cu^{2+}, one M^{2+} ion coordinates three of the four bipyridines present in each {**AB**}^{5,6} duplex to form a $[M(\mathbf{Bpy})_3]^{2+}$ complex with octahedral geometry, which is an unusual geometry for a complex formed inside a nucleic acid double helical structure. The lack of an inflection point in the titration curves monitored at 253, 304, or 314 nm for Cu^{2+}:{**AB**}^{5,6} = 1:1 is likely due to differences in the absorption coefficients for $[Cu(\mathbf{Bpy})_3]^{2+}$ and $[Cu(\mathbf{Bpy})_2]^{2+}$.

As the Ni^{2+} concentrations in the UV titrations increase beyond that of the {**AB**}^{5,6} duplex, a minor change is observed in the slope of the absorption at ~2:1 Ni^{2+}:{**AB**}^{5,6} ratio (Figure 4b). This small change suggests that the $[Ni(\mathbf{Bpy})_3]^{2+}$ complexes originally formed in the duplex may be converted into two $[Ni(\mathbf{Bpy})_2]^{2+}$ alternative base-pairs. For Cu^{2+}, the transformation of $[Ni(\mathbf{Bpy})_3]^{2+}$ into two $[Cu(\mathbf{Bpy})_2]^{2+}$ complexes is unambiguous. Indeed, the titration of the duplex with Cu^{2+} shows inflection points in the absorption at a 2:1 Cu^{2+}:{**AB**}^{5,6} ratio (Figure 4d), indicative of binding of one Cu^{2+} ion to each of the two pairs of bipyridine ligands. The absorption coefficient at 310 nm for $[Cu(\mathbf{Bpy})_2]^{2+}$ (Table 2) is in agreement with that measured for a synthetic $[Cu(bipy)_2]^{2+}$ complex (Table S2). This is also confirmed by the observation of different isosbestic points for Cu:{**AB**}^{5,6} ratios below and above 1:1 (Figure S4 a and b). Small changes in absorbance at 280 nm for Cu:{**AB**}^{5,6} ratios above 2:1 suggest that the $[Cu(\mathbf{Bpy})_2]^{2+}$ complexes may be further transformed into $[Cu(\mathbf{Bpy})]^{2+}$ complexes (Figures 4d and S4c).

Stoichiometry of Metal Binding to Bpy−PNA Duplexes that Contain Three Pairs of Bpy Ligands. Changes in the absorbance at 260 nm as a function of temperature between 95 and 20 °C for solutions containing a 1:1 mixture of **A**^{5,6,7} and **B**^{4,5,6} in the absence and presence of metal ions show a transition with low cooperativity and hyperchromicity (Figure 2b). This may be because either a duplex does not form or the hyperchromicity associated with the melting of an {**AB**}^{5,6,7} duplex with a limited number of nucleobase pairs is low. Therefore, we have conducted titrations of solutions that contain a 1:1 mixture of **A**^{5,6,7} and **B**^{4,5,6}, which have been slowly cooled from 95 °C, as it would be typically done in the preparation of PNA duplexes, and below, we

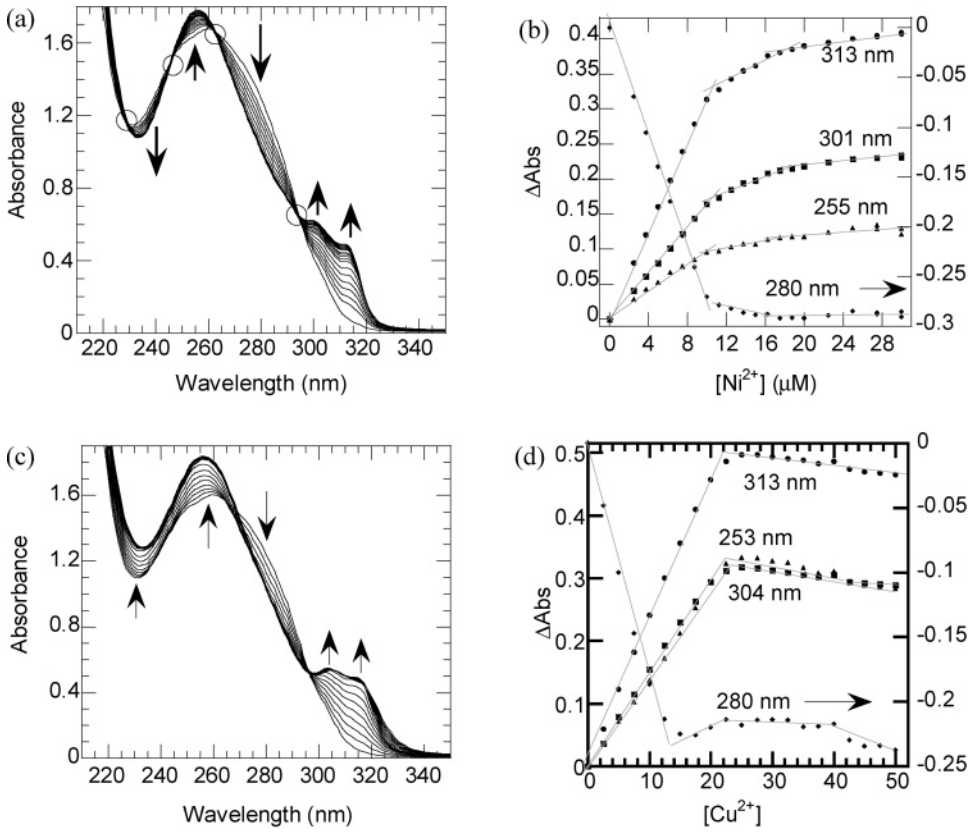

Figure 4. Titration of 10 μm {**AB**}^{5,6} in pH 7, 10 mM sodium phosphate buffer with Ni^{2+} (a and b) and Cu^{2+} (c and d).

Table 2. Stoichiometry and Absorption Coefficient at 310 nm for Complexes Formed between Metal Ions and **Bpy**−PNA Oligomers and Duplexes Based on M^{2+} Concentration at Inflection Points of UV Titrations

	Ni^{2+}				Cu^{2+}			
	M:PNA[a]	M:**Bpy**[a]	complex	ϵ_{310}[b]	M:PNA[a]	M:**Bpy**[a]	complex	ϵ_{310}[b]
A^{9}	1:2	1:2	[Ni(**Bpy**)$_2$]	27 000	1:2	1:2	[Cu(**Bpy**)$_2$]	20 700
					1:1	1:1	[Cu(**Bpy**)]	13 500
A^{5,6}	1:1	1:2	[Ni(**Bpy**)$_2$]	34 000	1:1	1:2	[Cu(**Bpy**)$_2$]	25 200
					2:1	1:1	[Cu(**Bpy**)]	13 200
A^{5,6,7}	1:1	1:3	[Ni(**Bpy**)$_3$]	40 000	1:1	1:3	[Cu(**Bpy**)$_3$]	33 300
{**AB**}^{9}	1:1	1:2	[Ni(**Bpy**)$_2$]	27 000	1:1	1:2	[Cu(**Bpy**)$_2$]	26 700
					2:1	1:1	[Cu(**Bpy**)]	13 900
{**AB**}^{5,6}	1:1	1:4	[Ni(**Bpy**)$_3$]	40 000	1:1	1:4	[Cu(**Bpy**)$_3$]	32 200
	2:1	1:2	[Ni(**Bpy**)$_2$]	25 000	2:1	1:2	[Cu(**Bpy**)$_2$]	24 500
{**AB**}^{5,6,7}	2:1	1:3	[Ni(**Bpy**)$_3$]	40 000	2:1	1:3	[Cu(**Bpy**)$_3$]	32 800
					6:1	1:1	[Cu(**Bpy**)]	12 220

[a] M:PNA is the M^{2+}:oligomer ratio for **A**^{n} strands or the M^{2+}:duplex ratio for {**AB**}^{n} systems. M:**Bpy** is the formal ratio between M^{2+} and **Bpy**. [b] These values were calculated from UV titration spectra without subtracting the absorbance at 310 nm for $[M^{2+}] = 0$. We have verified that the values calculated after subtraction of initial absorbance at 310 nm are very close to the ones listed in the table and lead to the same conclusions.

refer to the final state achieved in this process as {**AB**}^{5,6,7} duplexes.

In UV−vis titrations of {**AB**}^{5,6,7} duplexes with Ni^{2+} and Cu^{2+}, the absorption at 300−320 nm increases with the concentration of M^{2+} in solution and reaches a plateau for two metal ions per duplex (Figure 5). Isosbestic points are observed for both metal ions at concentrations for which M^{2+}:{**AB**}^{5,6,7} < 2:1. The absorption coefficient at 310 nm for the complexes formed at a ratio of Ni^{2+}:{**AB**}^{5,6,7} = 2:1 is 40 000 M^{-1} cm^{-1} (Table 2), which coincides with that for the synthetic $[Ni(bipy)_3]^{2+}$ complex (Table S2).[19] These data suggest the formation of two $[M(\mathbf{Bpy})_3]^{2+}$ complexes in each {**AB**}^{5,6,7} duplex, although we cannot exclude the possibility that each **A**^{5,6,7} or **B**^{4,5,6} strand forms one $[M(\mathbf{Bpy})_3]^{2+}$ complex.

A second small inflection point exists in the titration curves for {**AB**}^{5,6,7} at a Ni^{2+}:{**AB**}^{5,6,7} ratio of 3:1 (Figure 5b), which is suggestive of a conversion of $[Ni(\mathbf{Bpy})_3]^{2+}$ to $[Ni(\mathbf{Bpy})_2]^{2+}$ and of the existence of a triply metal-bridged {**AB**}^{5,6,7} duplex. Further support for this hypothesis comes from the fact that in titrations of **A**^{5,6,7} with Ni^{2+} no change in absorbance is observed after the $[Ni(\mathbf{Bpy})_3]^{2+}$ complex is formed (see below). The titrations of {**AB**}^{5,6,7} with Cu^{2+} clearly indicate that addition of Cu^{2+} in excess of two metal ions per {**AB**}^{5,6,7} duplex leads to binding of additional Cu^{2+} ions to the duplexes (Figure 5c and d). The absorbance

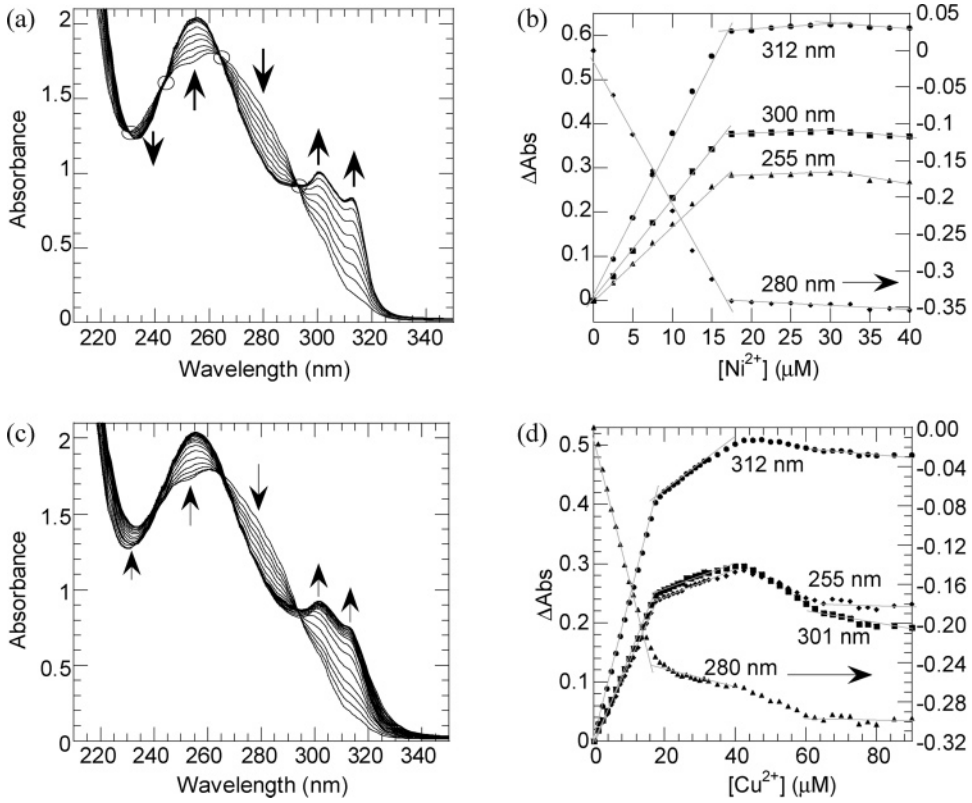

Figure 5. Titration of 10 μm {**AB**}^{5,6,7} in pH 7, 10 mM sodium phosphate buffer with Ni^{2+} (a and b) and Cu^{2+}(c and d). See Figure S4 for spectral changes at successive Cu^{2+} concentration regimes.

reaches a plateau for concentrations of Cu^{2+} at which Cu^{2+}:{**AB**}$^{5,6,7} \geq$ 6:1 (Figure 5d), which is suggestive of the formation of [Cu(**Bpy**)]$^{2+}$ complexes, in agreement with the results for {**AB**}^{9} and {**AB**}^{5,6}.

UV Titrations of Ligand-Containing PNA Oligomers. We have previously reported in the context of 8-hydroxyquinoline-modified PNA oligomers that strong coordinative bonds within a metal-containing alternative base pair can induce the hybridization of oligomers whose sequences are not completely complementary.[9] This could be the case for the partly self-complementary **A**^{9}, **A**^{5,6}, and **A**^{5,6,7}. It is also possible that given the presence of multiple ligands in **A**^{5,6} and **A**^{5,6,7} oligomers, they form intramolecular complexes with metal ions. To evaluate these possibilities for **A**^{9}, **A**^{5,6}, and **A**^{5,6,7}, we have performed UV titrations of the single strands.

Titrations of **A**^{9} with Ni^{2+} show isosbestic points at 225, 250, and 295 nm (Figures 6a). The absorbance at 280, 300, and 313 nm shows an inflection point for Ni^{2+}:**A**^{9} = 1:2 (Figure 6b). These observations indicate that an interstrand [Ni(**A**^{9})$_2$] complex forms upon addition of Ni^{2+} to **A**^{9}. The absorption coefficient for this complex at 310 nm is ~27 000 M^{-1} cm^{-1} (Table 2), which is close to the average of the values reported for [Ni(bipy)]$^{2+}$ and [Ni(bipy)$_3$]$^{2+}$ complexes (Table S2), supporting the formation of a [Ni(**Bpy**)$_2$]$^{2+}$ complex between two **A**^{9} strands.

Titrations of **A**^{9} with Cu^{2+} (Figure 7a) show distinct isosbestic points for Cu^{2+} concentrations for which Cu^{2+}:**A**^{9} is below 1:2 (i.e., 264 and 297 nm, Figure 8a) and between 1:2 and 1:1 (i.e., 230 and 250 nm, Figure 8b). These observations indicate that **A**^{9} forms different complexes with Cu^{2+} depending on the metal ion concentration. The changes in absorption as a function of the Cu^{2+} concentration (Figure 7b) confirm this hypothesis and indicate that [Cu(**Bpy**)$_2$]$^{2+}$ complexes form for Cu^{2+}:**A**^{9} < 1:2 and [Cu(**Bpy**)]$^{2+}$ complexes for Cu^{2+}:**A**^{9} > 1:2. The $\pi-\pi^*$ absorption bands of bipyridine in [Cu(**Bpy**)]$^{2+}$ are bathochromically shifted with respect to the corresponding bands for [Cu(**Bpy**)$_2$]$^{2+}$ (inset of Figure 8b). The absorption coefficient at 310 nm for the bands of [Cu(**A**^{9})] is close to the published value for synthetic [Cu(bipy)]$^{2+}$ (Table S2).[20] Thus, Cu^{2+} bridges the **A**^{9} strands into [Cu(**A**^{9})$_2$] complexes at low Cu^{2+} concentrations but coordinates to each strand to form [Cu(**A**^{9})]$^{2+}$ complexes at high concentrations. These results for titration of **A**^{9} with Ni^{2+} or Cu^{2+} are similar to those observed for titrations of the {**AB**}^{9} duplex, in that a [M(**Bpy**)$_2$]$^{2+}$ complex forms followed by its transformation to [Cu(bipy)]$^{2+}$ in the presence of excess Cu^{2+}.

Titrations of **A**^{5,6} with Ni^{2+} or Cu^{2+} indicate the formation of [M(**Bpy**)$_2$]$^{2+}$ complexes (Figures 6c and d and 7c and d) and are consistent with binding of either one metal ion to the two adjacent bipyridine ligands in each **A**^{5,6} strand or of two metal ions to pairs of **A**^{5,6} strands. The first process is intramolecular and thus entropically more favorable than the second one, although steric interactions may disfavor it. A thermal denaturation study of the partly complementary **A**^{5,6} strand (Chart 1) in the presence of one equivalent of Ni^{2+} per duplex revealed a cooperative transition with substantial hyperchromicity (data not shown), which suggests the formation of interstrand complexes.

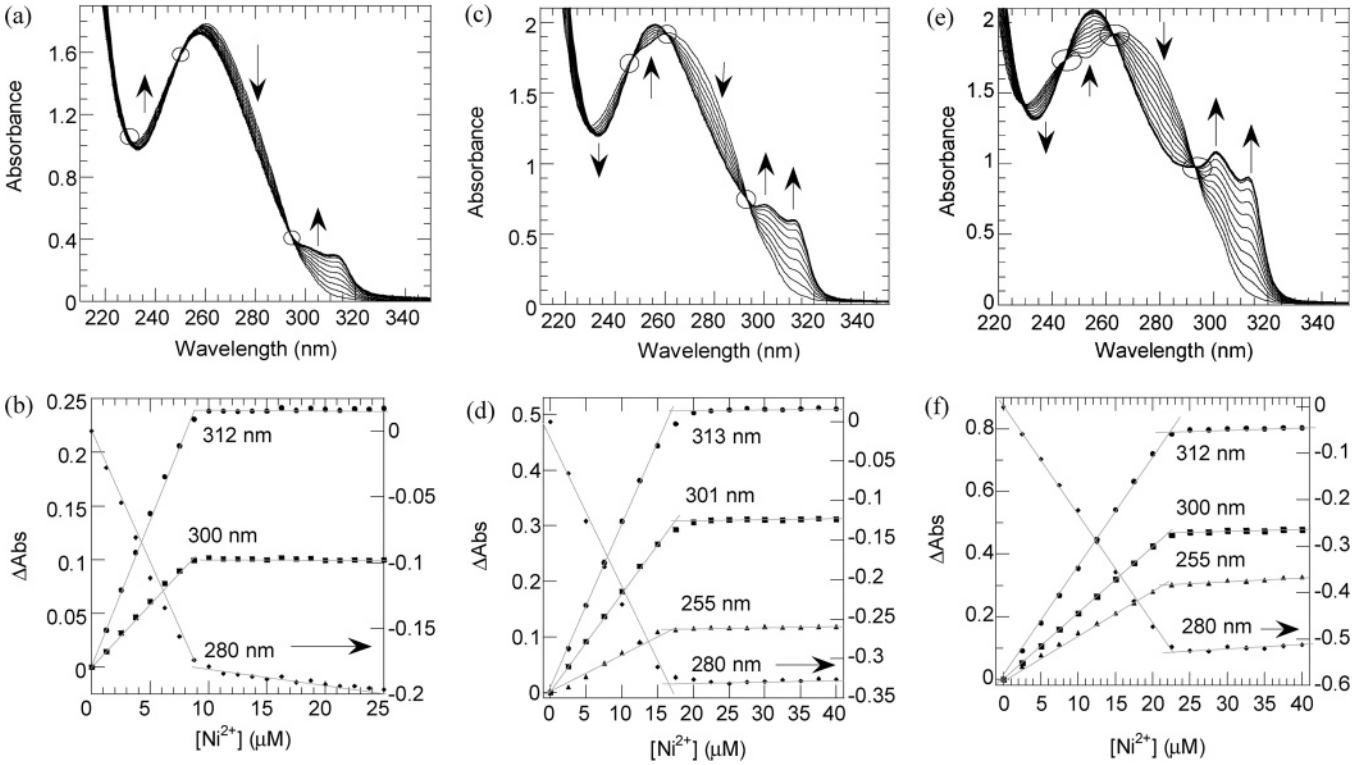

Figure 6. Spectrophotometric titration of 20 μM **A**[9] (a and b), 20 μM **A**[5,6] (c and d), and 20 μM **A**[5,6,7] (e and f) in pH 7, 10 mM sodium phosphate buffer with Ni^{2+}.

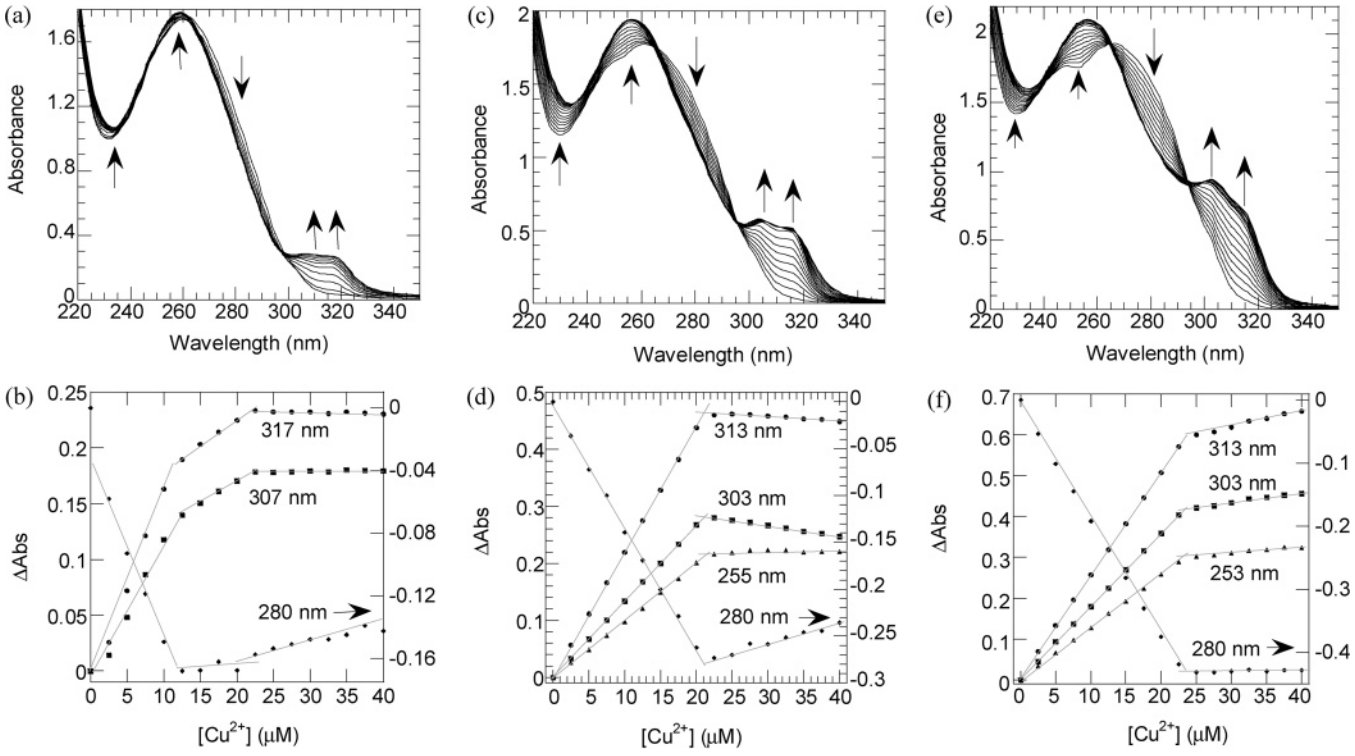

Figure 7. Spectrophotometric titration of 20 μM **A**[9] (a and b), 20 μM **A**[5,6] (c and d), and 20 μM **A**[5,6,7] (e and f) in pH 7, 10 mM sodium phosphate buffer with Cu^{2+}.

Titration of **A**[5,6] with Cu^{2+} shows different isosbestic points for Cu^{2+}:**A**[5,6] < 1:1 and for 1:1 < Cu^{2+}:**A**[5,6] < 1:2 (Figure S5). Upon the addition of more than 1 equiv of Cu^{2+} to **A**[5,6], a shift occurs in the position of the absorption maxima from 303 to 305 nm and from 314 to 315.5 nm. These changes suggest that the $[Cu(\mathbf{Bpy})_2]^{2+}$ complexes originally formed in the duplex transform into $[Cu(\mathbf{Bpy})]^{2+}$ ones, a hypothesis that is similar to that drawn on the basis of the results of titrations of **A**[9] and of bipyridine-modified {**AB**}[9] duplexes with Cu^{2+}. The direct formation of $[M(\mathbf{Bpy})_2]^{2+}$ complexes between **A**[5,6] and M^{2+} (M = Ni or Cu) is in contrast to the formation of $[M(\mathbf{Bpy})_3]^{2+}$ complexes between M^{2+} and

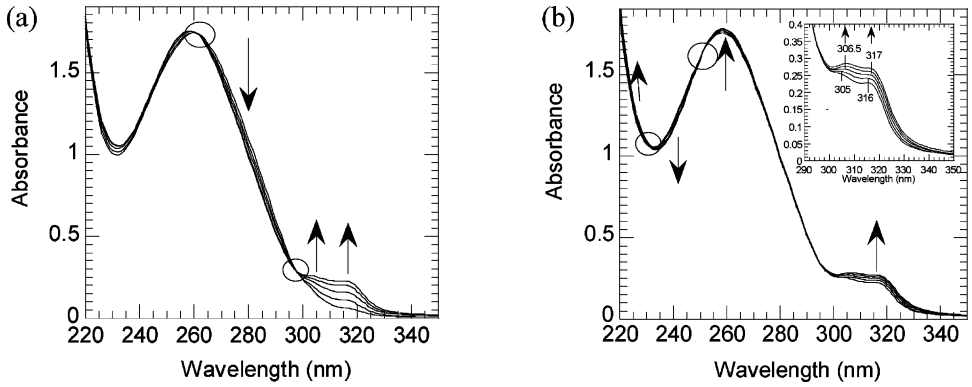

Figure 8. Spectrophotometric titration of 20 μM **A**[9] with Cu^{2+} for samples containing (a) up to 0.625 equiv of Cu^{2+}:PNA strand and (b) 0.625−1.125 equiv of Cu^{2+}:PNA strand. The inset shows the 280−320 nm range spectra for the same range of concentrations.

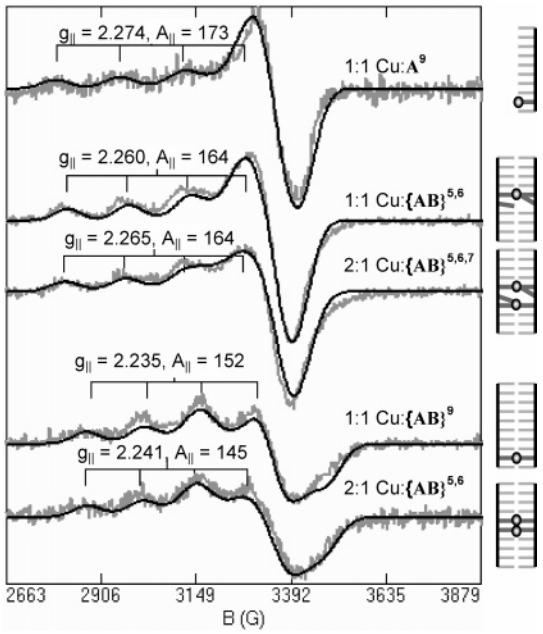

Figure 9. (left) EPR spectra of **Bpy**−PNA in the presence of Cu^{2+}. Hyperfine units are 10^{-4} cm^{-1}. (right) Cartoon representation of each Cu^{2+}−**Bpy**−PNA system (gray circles, Cu^{2+}; black vertical lines, PNA backbone; light gray lines, nucleobases; dark gray lines, **Bpy**).

{**AB**}[5,6]. This difference is indicative of a supramolecular chelate effect exerted by the duplex, which brings in close proximity four bipyridine moieties rather than only two, as is the case for each oligomer, and suggests that the complexes formed between M^{2+} and **A**[5,6] are intramolecular.

Titrations of **A**[5,6,7] strands that contain three adjacent bipyridine ligands with Ni^{2+} and Cu^{2+} clearly indicate the formation of $[M(\mathbf{Bpy})_3]^{2+}$ complexes (Figures 6e and f and 7e and f). Inflection points are observed in the titration curves at a M^{2+}:**A**[5,6,7] ratio of ∼1:1. Three isosbestic points are observed for titrations with Ni^{2+} (Figure 6e) and two isosbestic points are observed for titrations with Cu^{2+} below a Cu^{2+}:**A**[5,6,7] ratio of 1:1 (Figure S6a).

The stoichiometry of the M−**Bpy** complexes formed at a M^{2+}:**A**[5,6,7] ratio of 1:1 is consistent either with intrastrand tris-bipy complexes or the formation of two interstrand tris-bipy complexes by coordination of the transition metals to the six **Bpy** ligands of two PNA strands. When excess Cu^{2+} is added, small changes occur in the UV spectra (Figure S6b), suggesting that the original $[Cu(\mathbf{Bpy})_3]^{2+}$ complex undergoes further transformations, in contrast to titration with Ni^{2+} for which no such changes are observed. The lack of clear inflection points in the absorbance versus concentration curves for Cu^{2+}:**A**[5,6,7] between 1:1 and 3:1 prevented us from determining the stoichiometry of the complexes formed over this interval of concentrations (Figure 7f).

Gilmartin et al. have investigated the binding of Cu^{2+} to a trimer that had the same pseudo-peptide backbone as that of PNA and contained exclusively 4′-Me-2,2′-bipyridine ligands instead of nucleobases.[21] This PNA trimer is the closest comparison system for **A**[5,6,7] because it has a similar $(\mathbf{Bpy})_3$ fragment. Gilmartin et al. have reported that the trimer forms a double-stranded helicate in the presence of 3 equiv of Cu^{2+}, which contains three $[Cu(bipy)_2]^{2+}$ moieties. Our titrations do not allow us to determine if such a duplex forms for **A**[5,6,7]. This difference may be because $(\mathbf{Bpy})_3$ is flanked by nucleobases in **A**[5,6,7] but not in the PNA trimer, the point of bipyridine ligand attachment in the PNA trimer and in **A**[5,6,7] is different, or the concentration range used in the titration experiments is significantly different (i.e., <40 μM for **A**[5,6,7] and >700 μM for the PNA trimer).

EPR Spectroscopy. We have used EPR spectroscopy to further characterize the **Bpy**−PNA oligomers and duplexes in the presence of Cu^{2+}. Guided by the results of UV titrations, we prepared EPR samples with Cu^{2+}:PNA ratios that would lead to complexes with specific numbers of coordinated **Bpy**.

There is general agreement in the literature about the EPR parameters attributed to mono- and tris-bipyridine Cu^{2+} complexes, but some debate surrounds the existence and coordination geometry of bis-bipy complexes (Table S3). Noack and Gordon reported EPR studies of 60% H_2O−40% EtOH solutions containing a 1:2 ratio of Cu^{2+}:bipy at an unspecified pH.[22] They observed the coexistence of two Cu^{2+} complexes with different $g_{||}$ values and attributed them to the cis ($g_{||} = 2.23$) and trans ($g_{||} = 2.28$) isomers of $[Cu(bipy)_2L_2]^{2+}$ (L is a solvent molecule and will be omitted in future references to this complex). Walker and Sigel

(21) Gilmartin, B. P.; Ohr, K.; McLaughlin, R. L.; Koerner, R.; Williams, M. E. *J. Am. Chem. Soc.* **2005**, *127*, 9546−9555.
(22) Noack, M.; Gordon, G. *J. Chem. Phys.* **1968**, *48*, 2689−2699.

Table 3. EPR Parameters for Complexes Formed between Cu^{2+} and Bipyridine-Modified PNA in pH 7, 10 mM Sodium Phosphate Buffer, 25% Glycerol

PNA sample	Cu:bipy ratio	$g_{\|\|}$	$A_{\|\|}$ ($\times 10^{-4}$ cm^{-1})	$g_{\perp 1}$	$g_{\perp 2}$
A^{9}	1:1	2.274	173	2.063	2.055
{**AB**}^{5,6}	1:4	2.260	164	2.095	2.047
{**AB**}^{5,6,7}	1:3	2.265	164	2.111	2.048
{**AB**}^{9}	1:2	2.235	152	2.117	2.019
{**AB**}^{5,6}	1:2	2.241	145	2.113	2.030
{**AB**}^{5,6,7}	1:2	2.253	158	2.132	2.044

repeated the experiments of Noack and observed a different spectrum that they assigned to $[Cu(bipy)]^{2+}$ and $[Cu(bipy)_3]^{2+}$.[23] This did not exclude the presence of $[Cu(bipy)_2]^{2+}$ in solution, provided that it had spectral parameters similar to those of $[Cu(bipy)_3]^{2+}$. McKenzie suggested that the series of lines observed by Noack was due to $[Cu(bipy)_2]^{2+}$ complexes with different numbers of coordinated solvent molecules.[24] Marov et al. observed a spectrum similar to that attributed by Noack to *cis*-$[Cu(bipy)_2]^{2+}$ in either pH 2.2 60% H_2O−40% EtOH solutions or pH 8.5 borate buffer, in which the Cu^{2+}:bipy ratio was 1:2.[25] Recently, Garribba et al. concluded that when the Cu:bipyridine ratio is 1:2, *trans*-$[Cu(bipy)_2]^{2+}$ is the only species present in aqueous solutions and that a square pyramid *cis*-$[Cu(bipy)_2L]$ complex is present in 60% H_2O−40% EtOH solutions.[26] The EPR parameters for these complexes (Table S3 and Figure 10)[22,25,26] are used for comparison with those measured for complexes formed between Cu^{2+} and bipyridine-modified PNA (Table 3 and Figures 9 and 10).

Spectral parameters were determined from simulations of the EPR spectra (Figure 9) and are given in Table 3. This table is organized to group together Cu^{2+}−PNA complexes that have similar *g* and *A* values. As a consequence of this classification, the species appear also grouped by their formal Cu^{2+}:**Bpy** ratios. This is also apparent in the $A_{||}$ versus $g_{||}$ plot, which contains the values for Cu^{2+} complexes with **Bpy**−PNA and those for synthetic Cu^{2+}-bipyridine complexes (Figure 10).

The $g_{||}$ and $A_{||}$ values for the complex formed between Cu^{2+} and **A**^{9} in a 1:1 ratio are close to those reported for $[Cu(bipy)]^{2+}$ complexes (Table S3). The small difference between the $A_{||}$ values could be caused by weak binding by nearby nucleobases or buffer anions to Cu^{2+} or by steric interactions between the PNA oligomer and the $[Cu(\mathbf{Bpy})]^{2+}$ complex. This conclusion is in agreement with that drawn on the basis of UV titrations.

EPR spectra for the 1:1 Cu:{**AB**}^{5,6} and the 2:1 Cu:{**AB**}^{5,6,7} samples are similar to each other and have spectral parameters consistent with the formation of either *trans*-$[Cu(\mathbf{Bpy})_2]^{2+}$ or $[Cu(\mathbf{Bpy})_3]^{2+}$ (Figure 10 and Table S3). On the basis of the results of the UV titrations, we attribute the spectra to the existence of $[Cu(\mathbf{Bpy})_3]^{2+}$ in these samples.

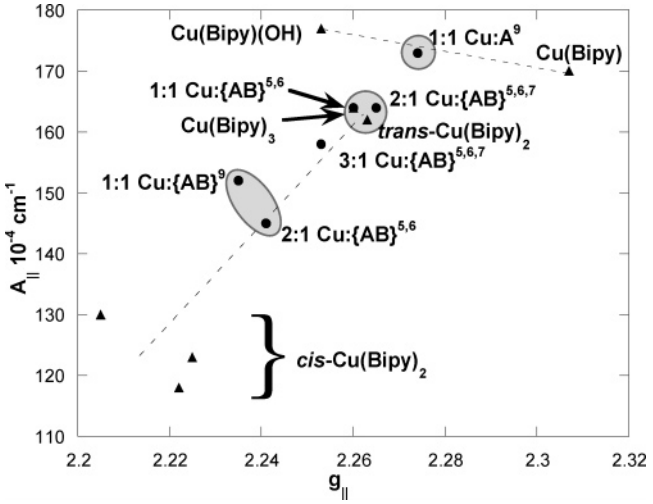

Figure 10. $A_{||}$ vs $g_{||}$ values for Cu^{2+} complexes with bipyridine (black triangles, Table S3) and with Bpy-modified PNA.

In solutions in which the Cu:{**AB**}^{9} ratio is 1:1 or the Cu:{**AB**}^{5,6} ratio is 2:1, the formal Cu:**Bpy** ratio is 1:2. The EPR spectra of these samples are similar to each other and are significantly different from those for $[Cu(\mathbf{Bpy})]^{2+}$ and $[Cu(\mathbf{Bpy})_3]^{2+}$ complexes formed with **Bpy**-modified PNA, and we assign them to $[Cu(\mathbf{Bpy})_2]^{2+}$ complexes, in agreement with the UV titration results. The $g_{||}$ and $A_{||}$ values are intermediate between those reported for *cis*- and *trans*-$[Cu(bipy)_2]^{2+}$. This difference could be caused by the binding of nearby nucleobases or solvent molecules to the otherwise four-coordinate Cu^{2+}complexes as observed for Cu^{2+}-coordinated ligand-modified DNA duplexes[4] or by the steric effect exerted by the PNA duplex on the metal complex.

The EPR spectra measured for a sample in which the Cu:{**AB**}^{5,6} ratio is 2:1 is slightly broader (line width = 400 G) than that observed for solutions containing Cu and {**AB**}^{9} in a 1:1 ratio (line width = 375 G), but no transitions are observed at $B \approx 1650$ mT, which would be characteristic of strong coupling between the two $S = 1/2$ Cu^{2+} ions. The broadening might be the consequence of weak dipolar coupling between the two $[Cu(\mathbf{Bby})_2]^{2+}$ complexes present in {**AB**}^{5,6}, but if this is the case, the coupling must be relatively weak. For example, if the complexes were at a distance of 6 Å at an angle of 30° between the normal to the ligands plane or at a distance of 5 Å at an angle of 45°, the splitting of the $g_{||}$ resonance caused by dipolar coupling would be ∼150 G, and the spectrum would be significantly broadened. This result indicates that the $[Cu(\mathbf{Bby})_2]^{2+}$ complexes are not stacked (expected distance 3.2−3.4 Å) but that, in a duplex containing multiple adjacent $[Cu(\mathbf{Bby})_2]^{2+}$ complexes, these complexes must be situated at distances larger than those between nucleobase pairs in PNA,[27,28] for example one in the minor groove and the other in the major groove of the duplex.

(23) Walker, F. A.; Sigel, H. *Inorg. Chem.* **1972**, *11*, 1162−1164.
(24) McKenzie, E. D. *Coord. Chem. Rev.* **1971**, *6*, 187−216.
(25) Marov, I. N.; Belyaeva, V. K.; Smirnova, E. B.; Dolmanova, I. F. *Inorg. Chem.* **1978**, *17*, 1667−1669.
(26) Garribba, E.; Micera, G.; Sanna, D.; Strinna-Erre, L. *Inorg. Chim. Acta* **2000**, *299*, 253−261.
(27) Rasmussen, H.; Kastrup, J. S.; Nielsen, J. N.; Nielsen, J. M.; Nielsen, P. E. *Nat. Struct. Biol.* **1997**, *4*, 98−101.
(28) Petersson, B.; Nielsen, B. B.; Rasmussen, H.; Larsen, I. K.; Gajhede, M.; Nielsen, P. E.; Kastrup, J. S. *J. Am. Chem. Soc.* **2005**, *127*, 1424−1430.

Table 4. EXAFS Curve Fitting Results for Bipyridine-Containing PNA in the Presence of Ni^{2+}

sample	Ni:bipy	N^a	R (Å)	σ^2 ($\times 10^{-3}$ Å^2)	R^b
A^{9}	1:1	4	2.06	2.4	40
{**AB**}^{5}	1:2	5	2.07	3.9	34
{**AB**}^{9}	1:2	5	2.06	3.9	21
A^{5,6}	1:2	5	2.07	3.2	110
{**AB**}^{5,6}	1:2	5	2.06	2.6	11
A^{5,6,7}	1:3	4	2.06	1.3	32
{**AB**}^{5,6}	1:4	5	2.06	2.0	143

[a] Integer coordination number giving the best fit. [b] Goodness of fit as $R = 1000 \times \sum_{i=1}^{N} (\chi_{icalcd}/\chi_{iobsd})^2$, where N is the number of data points.

Our titrations indicate that {**AB**}^{5,6,7} forms a mixture of complexes in the presence of 3 equiv of Cu^{2+}, some of which may be $[Cu(bipy)_2]^{2+}$. This conclusion is consistent with the EPR spectrum for this sample (not shown), which is very broad and has average $g_{||}$ and $A_{||}$ values that are intermediate between those observed for $[Cu(\mathbf{Bpy})_3]^{2+}$ and $[Cu(\mathbf{Bpy})_2]^{2+}$ complexes formed within PNA duplexes.

EXAFS of Bpy−PNA Systems in the Presence of Ni^{2+}. We have further attempted to obtain information about the coordination of the Ni^{2+}−**Bpy** complexes formed in PNA duplexes by using EXAFS and XANES. A comparison of the Fourier transformed EXAFS data for the set of Ni−PNA complexes (Figure S7) shows minor variations throughout the series. This is reflected in the curve fitting results, summarized in Table 4, where all Ni−N distances refine to approximately 2.06 Å, suggesting similar total coordination numbers in all of the complexes, and they do not allow us to be more precise than to say that the coordination number is 5 ± 1. Attempts to model the data with a heterogeneous first-coordination sphere, including varying contributions from nitrogen and oxygen scatterers, did not significantly improve the fits. The average first-shell Ni−N distances are consistent with the Ni−N distances for the compounds with $Ni(bipy)_2X_2$ or $Ni(bipy)_3$ coordination contained in the Cambridge Structural Database. These distances range from 2.05 to 2.11 Å, regardless of the identity of the X ligands. In an attempt to quantify the number of coordinated bipy ligands to a given Ni center, theoretical EXAFS data were generated from crystallographic data. The four prominent outer-shell scattering features predicted from the model structures, show an almost linear amplitude dependence on the number of coordinated bipyridines (Figure S7, bottom). In contrast, nearly all of the PNA spectra display a more complex pattern, and the lack of any simple trend in the outer-shell amplitudes precludes their use as a quantitative measure of metal coordination.

We have also examined the XANES spectra of the **Bby**-containing PNA strands and duplexes in the presence of Ni^{2+} (Figure S8a). The XANES region of the XAS spectrum is dominated by the electronic structure of the central atom. All seven Ni PNAs show weak 1s → 3d transitions, consistent with octahedral or four-coordinate square-planar geometry.[29] Comparison of the derivatives of XANES (Figure S8b), suggests that the complexes formed between Ni^{2+} and PNA fall into several categories. One category includes the duplexes {**AB**}^{5} and {**AB**}^{9} in the presence of one Ni^{2+} equivalent, which are expected to contain $[Ni(\mathbf{Bpy})_2]^{2+}$ complexes on the basis of UV titration results. The XANES of {**AB**}^{5,6} in the presence of 2 equiv of Ni^{2+} and of **A**^{5,6} in the presence of 1 equiv of Ni^{2+} are also similar to each other, which is in agreement with the fact that UV studies indicate that both samples contain $[Ni(\mathbf{Bpy})_2]^{2+}$ complexes. In the presence of 1 equiv of Ni^{2+}, **A**^{5,6,7} and {**AB**}^{5,6} are in the same, separate category, consistent with the fact that they form $[Ni(\mathbf{Bpy})_3]^{2+}$ complexes, based on the UV titration EPR spectroscopy.

Conclusions

The effect of ligand substitution of a natural base pair and subsequent metal binding is dependent on the position of the modification. The introduction of a ligand pair situated near the center of a PNA duplex significantly decreases the duplex's stability in contrast to a modification near the end of the duplex. Moreover, the stabilization exerted by metal ions on terminally modified duplexes surpasses the stabilization of duplexes with a central modification. This difference is the result of the base pairs at the end of the duplex being subject to fraying. The metal−ligand bonds reduce the fraying and significantly stabilize the duplex. The incorporation of multiple M^{2+}−**Bpy** moieties in the center of a PNA duplex does not grant greater thermal stability, probably because of electrostatic and steric interactions between adjacent, positively charged complexes.

Speciation diagrams for pH 7 aqueous solutions that contain bipyridine and Ni^{2+} in micromolar concentrations are shown in Figure 11. The distribution of species is changed when the bipyridines are incorporated in PNA. The oligomers to which **Bpy**s are attached are relatively bulky ligands and disfavor the formation of complexes with large coordination number, which would associate the metal ion with several PNA single strands. For example, the speciation diagrams indicate that $[Ni(bipy)_3]^{2+}$ is the dominant complex at a 1:3 Ni^{2+}:bipyridine ratio (Figure 11a), whereas titration of **A**^{9} with Ni^{2+} revealed that $[Ni(\mathbf{A}^{9})_2]$ is the dominant species at a 1:3 Ni^{2+}:**A**^{9} ratio (Figure 6a and b).

On the other hand, oligomers that contain multiple adjacent **Bpy** monomers bring several ligands in close proximity to each other and exert a chelate effect, which favors the formation of complexes in which the metal ion coordinates the maximum number of accessible ligands. For example, titration of either **A**^{5,6,7} or {**AB**}^{5,6,7} with Cu^{2+} leads to the formation of $[Cu(\mathbf{Bpy})_3]^{2+}$ at a Cu^{2+}:oligomer ratio of 1:1, in contrast to the behavior indicated by speciation diagrams, namely, at micromolar concentrations, $[Cu(bipy)_3]^{2+}$ is a minority species irrespective of the Cu^{2+}:bipyridine ratio (Figure 11b). In another example, titration of **A**^{5,6}, which contains two adjacent bipyridine ligands, leads to $[Ni(\mathbf{Bpy})_2]^{2+}$ for formal Ni^{2+}:**Bpy** ratios up to 1:2, whereas speciation diagrams predict that, beyond a Ni^{2+}:bipy ratio of 1.25:1, $[Ni(bipy)]^{2+}$ is the major complex.

(29) Colpas, G. J.; Maroney, M. J.; Bagyinka, C.; Kumar, M.; Willis, W. S.; Suib, S. L.; Mascharak, P. K.; Baidya, N. *Inorg. Chem.* **1991**, *30*, 920−928.

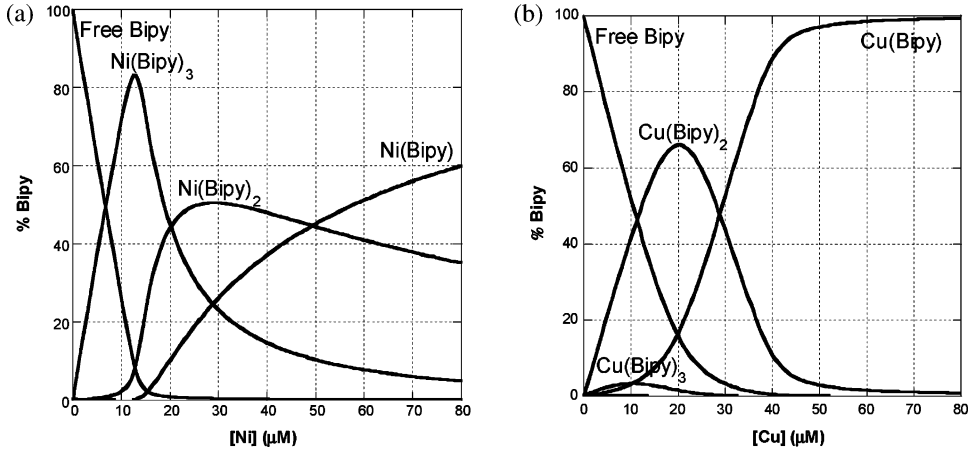

Figure 11. Speciation diagrams for (a) Ni^{2+}−bipy and (b) Cu^{2+}−bipy pH 7 solutions. The bipyridine concentration was 40 μM. Binding and acidity constants used in constructing the speciation diagrams were obtained from ref 30 and 31 (Table S4).

A supramolecular chelate effect occurs when hybridization of complementary PNA oligomers brings **Bpy** ligands in close proximity. For example, titration of {**AB**}[5,6] with Ni^{2+} leads to the formation of $[Ni(\mathbf{Bpy})_3]^{2+}$ if the Ni^{2+}:**Bpy** ratio is 1:4, but **A**[5,6] forms $[Ni(\mathbf{Bpy})_2]^{2+}$ complexes at the same Ni^{2+}:**Bpy** ratio. The same relationship was observed in titrations of {**AB**}[5,6] or **A**[5,6] with Cu^{2+}. This duplex-promoted chelate effect has been previously documented for metal incorporation in ligand-modified DNA and PNA duplexes. $[Ag(pyridine)_2]^+$ complexes were formed within a 21-bp pyridine-containing DNA duplex at which the same complexes would not form between Ag^+ and isolated pyridine.[7] In another example of a chelate effect exerted by a duplex, titrations of PNA duplexes containing one pair of 8-hydroxyquinoline (**Q**) ligands lead to the formation of $[Cu\mathbf{Q}_2]$ complexes both at low and high temperature, but these complexes can be transformed into [Cu**Q**] complexes in the presence of excess Cu^{2+} only at high temperatures at which the duplex is dissociated.[9]

Importantly, the charge and geometry of adjacent, intraduplex metal−ligand moieties affects the stability of the duplex upon metal binding. In titrations of {**AB**}[5,6,7], we find clear evidence that nickel ions coordinate to the duplex or separated strands to form $[Ni(\mathbf{Bpy})_3]^{2+}$ complexes, but our data does not prove that in the presence of a third equivalent of Ni^{2+}, three $[Ni(\mathbf{Bpy})_2]^{2+}$ complexes can be generated in {**AB**}[5,6,7] duplexes. In contrast, up to five Cu^{2+} ions were shown to coordinate to hydroxypyridone-modified DNA duplexes to form five adjacent [Cu(hydroxypyridone)$_2$] alternative base pairs.[15] A difference between the metal binding to bipyridine-modified PNA duplexes and hydroxypyridone-modified DNA duplexes is expected because the $[Ni(bipy)_n]^{2+}$ complexes are positively charged while the [Cu(hydroxypyridone)$_2$] complexes are neutral. Furthermore, hydroxypyridone forms planar complexes with Cu^{2+} in solution, whereas bipy and Ni^{2+} or Cu^{2+} form octahedral or distorted square-planar complexes, with the typical distortions from square planarity for $[M(bipy)_2]$ complexes being either twist or bow-step (Scheme 3).[32] Electrostatic repulsion may prevent the binding of several metal ions in adjacent positions in the duplex. For this reason, DNA, which has a negatively charged backbone, may be a better choice for the incorporation of positively charged complexes. Indeed, a DNA duplex modified to incorporate three adjacent $[NiL_2]^{2+}$ complexes forms, and it is more stable in the presence of 3 equiv of the metal ion than in the presence of two equivalents of Ni^{2+}.[16]

This study brings evidence that ligand-modified PNA oligomers and duplexes can be used to organize several metal ions in close proximity to each other within PNA. These results and their comparison to those obtained by others for ligand-modified DNA indicate that ligand affinity for metal ions, the geometry and charge of the metal complexes, and the charge of the nucleic acid must be considered carefully in the design of such systems. EPR spectroscopy studies suggest that even when two metal ions coordinate to a PNA duplex in which two bipyridine pairs are next to each other, the two metal−ligand complexes are far enough from each other that dipolar coupling is very weak. This conclusion indicates that for applications of metal-containing PNA duplexes for which intermetal interactions are important, electrostatic and steric repulsion between the metal complexes must be minimized or the metal ions must be bridged by ligands.

Experimental Section

Synthesis of the PNA Monomer 4. 2,2′-Bipyridine-5-acetic acid **1** was obtained according to previously published procedures (Scheme 4).[12,33] All other chemicals were purchased from commercial sources and were used without further purification.

Aeg (0.825 g, 3 mmol) was dissolved in 10 mL of DMF. To this solution, 0.54 g (3.3 mmol) of DhBtOH and 0.76 g (3.3 mmol) of 2,2′-bipyridine-5-acetic acid (**1**) were added along with 10 mL of DCM. The solution was cooled to 0 °C, and 0.745 g (3.6 mmol) of DCC was added. The reaction mixture was stirred vigorously at 0 °C for 1.5 h, followed by stirring at room temperature for 3 h.

(30) Martell, A. E.; Smith, R. M. *Critical Stability Constants*; Plenum: New York, 1982; Vol. 5, First Supplement.

(31) Smith, R. M.; Martell, A. E. *Critical Stability Constants, Vol. 4: Inorganic Complexes*; Plenum: New York, 1976.

(32) Milani, B.; Anzilutti, A.; Vicentini, L.; Santi, A. S.; Zangrando, E.; Geremia, S.; Mestroni, G. *Organometallics* **1997**, *16*, 5064−5075.

(33) Ballardini, R.; Balzani, V.; Clemente-Leon, M.; Credi, A.; Gandolfi, M. T.; Ishow, E.; Perkins, J.; Stoddart, J. F.; Tseng, H.-R.; Wenger, S. *J. Am. Chem. Soc.* **2002**, *124*, 12786−12795.

Scheme 4. Synthesis of 2,2′-Bipyridine-5-acetic acid

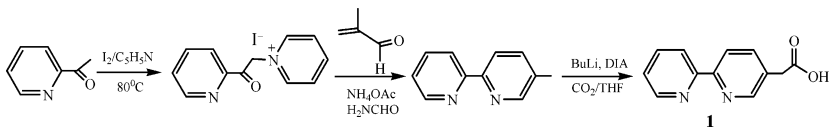

1

The finely powdered white solid precipitate formed during stirring was removed by filtration and washed with 10 mL of DCM. To the combined filtrate, 30 mL of DCM was added, and the solution was washed successively with dilute aqueous $NaHCO_3$ (3 × 20 mL), $KHSO_4$ (2 × 25 mL), and finally, with brine (2 × 30 mL). The organic phase was dried over anhydrous Na_2SO_4 and filtered. The solvent was evaporated to a final volume of 5 mL. White solid DCU precipitated and was discarded. To the new filtrate, 20 mL of hexanes was added, and the reaction mixture was refrigerated (4 °C) overnight. The yellow solid **3**, which precipitated, was dried under vacuum. Yield: 1.06 g (75%). ^{1}H NMR (500 MHz, in CD_3SOCD_3): δ 8.74 (1H, s), 8.60 (ma) and 8.54 (mi) (1H, s), 8.46−8.33 (m, 2H), 7.97 (1H, m), 7.82 (m, 1H), 7.48 (t, 1H), 7.07 (1H, br. NH), 4.32 (mi) and 3.97 (ma) (2H, s), 3.90 (ma) and 3.75 (mi) (2H, s), 1.45−1.39 (18H, 2xs, Boc + O*t*Bu). ES-MS (CH_3CN): m/z = 471.07 (MH^+, 100%).

The monomer ester **3** was hydrolyzed following a previously reported procedure.[12] **3** (0.470 g, 1 mmol) was taken up in a mixture of 1:2 ethanol/water (28.5 mL). To this suspension, a concentrated aqueous solution of NaOH (25 M, 0.5 mL) was added. The mixture was stirred at room temperature for 6 h. Then the resulting clear yellow solution was filtered and carefully acidified to pH 3 by the addition of 4 M HCl and extracted with 3 × 50 mL of ethyl acetate. The ethyl acetate fractions were combined, dried over Na_2SO_4, and filtered. The solvent was evaporated to yield an orange yellow solid, which was dried under vacuum overnight to obtain a bright yellow product **4**. Yield: 0.26 g (63%). mp: 132−135 °C. ^{1}H NMR (300 MHz, in $CDCl_3$): δ 8.78 (1H, d), 8.62 (s, 1H), 8.31 (dd, 2H), 7.84 (dd, 2H), 7.33 (1H, t), 5.6 (1H, br NH), 4.18 (mi) and 4.05 (ma) (2H, s), 3.84 (ma) and 3.68 (mi) (2H, s), 3.49 (2H, m, CH_2), 3.27 (2H, t, CH_2), 1.44−1.37 (9H, s, Boc). ES-MS (CH_3CN): m/z = 415.0 (MH^+, 100%).

Solid-Phase PNA Synthesis. PNA oligomers were synthesized on a 10 μmol scale, using a standard Boc-protection strategy.[17,34] As a solid support, cross-linked polystyrene beads functionalized with 4-methylbenzhydrylamine were used (200−400 mesh 0.18 mequiv/g, Peptides International, Louisville, KY). An L-lysine residue was preloaded onto the resin using Boc-Lys(2-Cl-Z)-OH (Peptides International) by standard procedure to lower the loading to between 0.10 and 0.05 mequiv/g.[34] Boc-protected PNA monomers were purchased from Applied Biosystems (Foster City, CA) and used without further purification. HBTU (Applied Biosystems) was used as coupling agent, and coupling time was typically 30 min. The coupling of the second or third **Bpy** monomers required longer times (1 h). PNA oligomers were cleaved from solid-support using *m*-cresol/thioanisole/TFMSA/TFA (1:1:2:6) and precipitated with cold diethyl ether. PNA strands were purified by reverse-phase HPLC using a C18 column (5 μm; 19 × 100 mm; Waters Corporation, Milford, MA) and were subsequently lyophilized for long-term storage. Characterization of the oligomers was performed by MALDI-TOF (Table 5) on an Applied Biosystems Voyager Biospectrometry Workstation using α-cyano-4-hydroxycinnamic acid matrix (10 mg/mL in 1:1 water/acetonitrile, 0.1% TFA).

Thermal Denaturation Studies. Hybridization experiments were performed by measuring the change in absorbance at 260 nm corresponding to the $\pi-\pi^*$ transitions of the nucleobases. Concomitantly, the change in absorbance at 315 nm was recorded to visualize the temperature dependence of metal binding to the bipyridine moiety. A Varian Cary 300 spectrophotometer equipped with a thermoelectrically controlled, multicell holder was used for the thermal denaturation studies. All samples were prepared by mixing stoichiometric amounts of PNA strands in 10 mM phosphate buffer (pH 7) to give a total strand concentration of 10 μM, which corresponds to a 5 μM duplex concentration. The concentration of the stock solution was determined by UV absorption at 95 °C using the extinction coefficients of the corresponding monomers given in the literature.[17] The extinction coefficient for the bipyridine monomer (ϵ_{260} = 9770 M^{-1} cm^{-1} at pH 7) was determined from the slope of the calibration curve A_{260} vs the concentration of the monomer acid, **4**. UV melting curves were recorded for both cooling and heating modes at the rate of 1 °C/min. The recorded spectra were smoothed using an adjacent-point averaging algorithm with a 5-point window. The melting temperature (T_M) was defined as the maximum of the melting curve's first derivative. For all three metal ions, the melting temperature has been estimated on the basis of the temperature dependence of absorbance at 260 nm.

Table 5. Mass Characterization of **Bpy**−PNA Oligomers

name	sequence	calcd *m*/*z*	exptl *m*/*z*
A[9]	Lys-C**Bpy**TCTAGTGA	2877	2888
B[2]	Lys-TCACTAGA**Bpy**G	2886	2886
A[5,6]	Lys-CATC**BpyBpy**GTGA	2907	2907
B[5,6]	Lys-TCAC**BpyBpy**GATG	2907	2908
A[5,6,7]	Lys-CATB**BpyBpy**GTGA	2952	2953
B[4,5,6]	Lys-TCAC**BpyBpyBpy**ATG	2912	2914

UV Titrations. The UV spectra between 315 and 220 nm were recorded on a Varian Cary 50 spectrophotometer as a function of the metal concentration. Solutions for titrations contained a total PNA strand concentration of 20 μM in 10 mM phosphate buffer (pH 7); the samples were annealed prior to titrations by slow cooling from 95 to 20 °C. UV titrations were carried out by addition of standard 500 μM metal solutions and were continued after reaching equilibrium. Kinetics studies showed that metal binding to the bipyridine-modified PNA oligomers and duplexes occurs within 10 min (Figures S9 and S10). The ΔAbs values were obtained by correcting the absorbance measured after each addition for dilution and PNA absorption.

EPR Spectroscopy. EPR spectra were recorded on an X-band (9.6 GHz) Bruker ESP 300 spectrometer equipped with an Oxford ESR 910 cryostat. The microwave frequency was calibrated with a frequency counter and the magnetic field with a NMR gaussmeter. The temperature was calibrated using devices from Lake Shore Cryotronics. Spectra were collected under nonsaturating conditions. Samples were prepared in pH 7.0, 10 mM sodium phosphate buffer with 25% glycerol as a glassing agent in the presence of $CuCl_2$ or $Cu(NO_3)_2$. Samples containing PNA and Cu^{2+} in an appropriate molar ratio were heated at 95 °C for 10 min, slowly cooled to room temperature, transferred into EPR tubes, and frozen in liquid nitrogen. EPR spectra were simulated using the program SpinCount written by Prof. Michael P. Hendrich.[35] Spin quantitation was done relative to a 0.499 mM Na_2[Cu(edta)] standard, the copper concentration of which was determined by plasma emission spectros-

(34) Koch, T. In *Peptide Nucleic Acids*, 2nd ed.; Nielsen, Ed.; Horizon Bioscience: Hethersett, Norwich, U.K., 2004; pp 37−59.

copy. Spectra were obtained at 12 K with a microwave frequency of 9.65 GHz ($B_1 \perp B$).

X-ray Absorption Spectroscopy. PNA samples, containing 10% (v/v) glycerol added as a glassing agent, were loaded in Lucite cuvettes with 6 μm polypropylene windows and frozen rapidly in liquid nitrogen. X-ray absorption spectra were measured at the National Synchrotron Light Source (NSLS), beamline X9B, with a Si(111) double-crystal monochromator. Fluorescence excitation spectra were measured with a 13-element solid-state Ge detector array, and samples were held at ~15 K in a Displex cryostat. X-ray energies were calibrated by reference to the absorption spectrum of a Ni foil, measured concurrently with the PNA spectra. XANES spectra were normalized by fitting polynomials to the data below and well above the edge, setting the edge jump equal to 1.

EXAFS data were processed using the program SixPack, available free of charge from http://www-ssrl.slac.stanford.edu/~swebb/index.htm. EXAFS spectra were Fourier transformed over the range $k = 1-13.6$ Å^{-1} ($E_0 = 8360$ eV). The first shell [$\Delta R = 0.8-2.1$ Å] was reverse Fourier transformed over the same k-range. The Fourier-filtered first-shell EXAFS data were fit to eq 1 using the nonlinear least-squares engine of IFEFFIT that is distributed with SixPack (IFEFFIT is open source software available from http://cars9.uchicago.edu/ifeffit).

$$\chi(k) = \sum \frac{N_{as} A_s(k) S_c}{kR_{as}^2} \exp(-2k^2\sigma_{as}^2) \exp(-2R_{as}/\lambda) \sin[2kR_{as} + \phi_{as}(k)] \quad (1)$$

In eq 1, N_s is the number of scatterers within a given radius (R_{as}, $\pm \sigma_{as}$), $A_s(k)$ is the backscattering amplitude of the absorber−scatterer (as) pair, S_c is a scale factor, $\phi_{as}(k)$ is the phase shift experienced by the photoelectron, λ is the photoelectron mean free path, and the sum is taken over all shells of scattering atoms included in the fit. Theoretical amplitude and phase functions, $A_s(k)$ $\exp(-2R_{as}/\lambda)$ and $\phi_{as}(k)$, were calculated using FEFF version 8.00.[36] The Ni−N scale factor, S_c in eq 1, and the threshold energy, ΔE_0, were held fixed at 0.8 and −20 eV, respectively. Fits to PNA data were then obtained for all reasonable coordination numbers, varying only R_{as} and σ_{as}^2. In an attempt to quantify the number of bipy ligands per nickel ion, we compared outer-shell scattering from bipy ligands in the PNA complexes to the calculated EXAFS of three crystallographically characterized complexes, generated by using the crystallographic coordinates of each compound as input to FEFF. The complexes used were (CCDC codes mono-bipy = CUPJEC, bis-bipy = GOLSUV, and tris-bipy = WADBOT), which include only water molecules as ancillary ligands.

Acknowledgment. The National Synchrotron Light Source is supported by the U. S. Department of Energy. The Achim Group is grateful to the National Science Foundation (CHE-0347140) and the Camille and Henry Dreyfus Foundation for financial support of this research. NMR spectra were recorded on instruments purchased with an NSF grant (CHE-0130903). MALDI-TOF and ES mass spectrograms were recorded in the Center for Molecular Analysis at Carnegie Mellon University, which is supported by NSF grants CHE-9808188 and DBI-9729351. We thank Dr. Sebastian A. Stoian for his assistance with collection of the EPR spectra and Hyewon Youm and Delia Popescu for work in the preliminary stages of this project.

Supporting Information Available: Figures showing UV spectra, melting curves, spectrophotometric titration, Fourier transforms, XANES, and kinetics and tables of binding constants, UV bands, EPR parameters for the compounds studied in this paper. This material is available free of charge via the Internet at http://pubs.acs.org.

IC0609610

(35) Hendrich, M. P.; Petasis, D.; Arciero, D. M.; Hooper, A. B. *J. Am. Chem. Soc.* **2001**, *123*, 2997−3005.

(36) Ankudinov, A. L.; Ravel, B.; Rehr, J. J.; Conradson, S. D. *Phys. Rev. B* **1998**, *58*, 7565−7576.